Schottky noise in a laser-cooled ion beam

V. A. Lebedev, J. S. Hangst, and J. S. Nielsen

Institute of Physics and Astronomy, Aarhus University, Aarhus, Denmark

(Received 2 February 1995)

The application of the general theory of Schottky noise to a beam subjected to laser cooling in a storage ring is considered. It is shown that the noise properties differ strongly from the case of an electron-cooled beam. The important role of the tails of the velocity distribution is discussed. Good agreement between the theoretical predictions and experimental results obtained at the ASTRID storage ring has been found. The possibility of extracting dynamical information from the Schottky spectra is also discussed.

PACS number(s): 41.75.Ak, 29.20.Dh, 29.27.Bd, 52.25.Wz

I. INTRODUCTION

Several methods of nondestructive beam diagnostics based on the analysis of signals induced by the beam on pickup electrodes have been widely used in accelerators. In particular, the study of beam thermal noise (Schottky noise) is one of the most commonly used methods for measuring properties of a continuous beam. During the last 15 years this technique has been routinely used at practically every installation operating with continuous beams, including the antiproton accumulators at CERN and Fermilab, and a number of installations with comparatively low energy beams used for experiments in atomic and nuclear physics [1].

In this article we will analyze the case of longitudinal particle motion, where the fluctuations of the total number of particles inside a pickup electrode are measured. The signal from a single particle has the form of a short pulse that is repeated at the rotation frequency; thus, the spectral density of the beam noise consists of narrow peaks located at the harmonics of the revolution frequency.

If the beam density is small or if the beam has a sufficiently large momentum spread, so that the collective beam interaction is small enough, one can consider the motion of separate particles to be independent. Then the noise spectral density around each harmonic, $S_n(\delta\omega_n)$, is directly related to the particle distribution function in revolution frequency [1,3],

$$S_n(\delta\omega_n) = \frac{N}{n} f_\omega(\delta\omega_n/n), \quad \delta\omega_n = \omega - n\omega_0 , \qquad (1)$$

and one can easily measure the momentum distribution function and calculate the rms momentum spread in the beam. Here $f_\omega(\delta\omega)$ is the particle distribution function in revolution frequency normalized so that $\int f_\omega(\delta\omega)d\delta\omega = 1$, N is the number of particles in the beam, and n is the harmonic number. One can see from Eq. (1) that the integral of the spectral density around each peak is equal to the number of particles and does not depend on other parameters.

In a dense and cold beam the motion of each particle is strongly influenced by the motion of other particles; thus the noise spectral density should be determined by the particle interactions. The general theory of such fluctuations was developed in plasma physics [2] and successfully applied to accelerators in Ref. [3], which we will follow here. For the most frequently encountered case, when the beam energy is below the transition energy and the main contribution to the ring impedance is from Coulomb repulsion, the noise spectral density should be strongly suppressed by particle interactions. In this case the spectrum around each harmonic usually consists of two peaks located symmetrically around this harmonic. These peaks are associated with charge density waves propagating upstream and downstream along the beam. It was shown [3] that in the equilibrium state, when the velocity distribution function is Gaussian, the integral of the spectral density around each harmonic is equal to

$$\langle A_n^2 \rangle = \int_{\substack{\text{around} \\ \text{harmonic}}} S_n(\omega)d\omega = N\frac{\overline{\delta\omega^2}}{\overline{\delta\omega^2} + \Omega^2} . \qquad (2)$$

Here $\overline{\delta\omega^2}$ is the rms spread of the particle revolution frequencies, Ω is the so-called coherent shift, and we use the same normalization of the longitudinal beam density as in Ref. [3],

$$\rho(\theta,t) = \frac{1}{2\pi} \sum_{n=-\infty}^{n} A_n(t)e^{in(\omega_0 t - \theta)}, \quad \int_0^{2\pi}\rho(\theta,t)d\theta = N . \qquad (3)$$

For purely capacitive impedance (Coulomb particle repulsion) Ω is equal to the relative frequency at which these coherent waves in the beam propagate around the ring. One can see that for a cold beam, when $\overline{\delta\omega^2} < \Omega^2$, the fluctuations are strongly suppressed by the particle interaction.

This noise suppression was studied theoretically and experimentally for the first time in Novosibirsk for an electron-cooled beam [3,4]. Good agreement between theory and experiment was found. But recently, experiments with laser cooling have exhibited a very strong discrepancy between the developed theory and experimental results [5]. In particular, it was found that after

switching on the cooling, the noise spectral density, instead of decreasing, increased by two orders of magnitude. This article is devoted to an analysis of this phenomenon.

II. REVIEW OF THE THEORY

We will follow Ref. [3], modified only as necessary to correct obsolete definitions and minor inconsistencies. There it was shown that the noise spectral density around the nth harmonic of the revolution frequency is equal to

$$S_n(\delta\omega_n) = \frac{N}{n} \frac{f_\omega(\delta\omega_n/n)}{|\varepsilon_n(\delta\omega_n)^2|}, \quad \delta\omega_n = \omega - n\omega_0, \quad (4)$$

where $\varepsilon_n(\omega)$ is the analog of the plasma dielectric permittivity. For the case of a beam without collisions, it can be expressed through the integral of the distribution function

$$\varepsilon_n(\omega) = 1 + \frac{\Omega_n^2}{n} \int_{-\infty}^{\infty} \frac{1}{\omega - n\omega' - i0} \frac{\partial f_\omega(\omega')}{\partial\omega'} d\omega'. \quad (5)$$

The contour used for the integral includes the real axis and is deformed around the pole at $\omega' = \omega/n$ above the real axis. Here the coherent shift for the n-th harmonic is determined by

$$\Omega_n^2 = i\frac{NZ^2e^2\omega_0}{4\pi^2\bar{R}} \frac{d\omega}{dp} nZ_n, \quad \frac{d\omega}{dp} = \frac{\omega_0}{p_0}\left[\frac{1-\alpha\gamma^2}{\gamma^2}\right], \quad (6)$$

where N is the number of particles in the beam and eZ is their charge, $\bar{R}$ is the average ring radius, $\alpha \equiv p/\omega(d\omega/dp)$ is the momentum compaction factor, and Z_n is the longitudinal ring impedance for harmonic n. The coherent shift Ω_n is the characteristic frequency describing the time evolution of a density perturbation having the wavelength $2\pi\bar{R}/n$. In general, the impedance Z_n has both real (resistive) and imaginary (capacitive and inductive) parts.

One can see that in the case of a hot and weak beam the beam permittivity is close to 1, $\varepsilon \approx 1$, and Eq. (4) coincides with Eq. (1). It should be noted that Eq. (4) can be used only if a beam is stable, i.e., all roots of the dispersion equation

$$\varepsilon_n(\omega) = 0 \quad (7)$$

have positive imaginary parts.

Usually, for low energy beams, Coulomb repulsion produces the main contribution to the storage ring impedance. In this case the impedance is purely capacitive and is given by [6]

$$\frac{Z_n}{n} = \frac{4\pi}{c\beta\gamma^2 i}\left[\ln\frac{r_c}{r_b} + \frac{1}{2}\right], \quad (8)$$

where β and γ are the relativistic factors, c is the velocity of light, and r_c and r_b are the radii of the vacuum chamber and the beam, respectively. Thus, for beams below transition energy $\alpha\gamma^2 < 1$, the square of the coherent shift becomes real and positive,

$$\Omega^2 \equiv \frac{\Omega_n^2}{n^2} = \frac{NZ^2e^2(1-\alpha\gamma^2)}{\pi M\bar{R}^3\gamma^5}\left[\ln\frac{r_c}{r_b} + \frac{1}{2}\right]. \quad (9)$$

[Note that the value for the square of the coherent shift presented in Ref. [3] is two times smaller than that determined by Eq. (9). This mistake is corrected in [8], the English edition of which will be published soon.]

For a Gaussian distribution function

$$f_\omega(\omega) = \frac{1}{\sqrt{2\pi}\sqrt{\delta\omega^2}}\exp\left[-\frac{\omega^2}{2\delta\omega^2}\right], \quad (10)$$

the integral (5) can be reduced to the following expression [7]:

$$\varepsilon_n(\omega) = 1 + \frac{\Omega_n^2}{n^2\delta\omega^2}\left[1 - 2ye^{-y^2}\int_0^y e^{-x^2}dx\right.$$
$$\left. - i\sqrt{\pi}ye^{-y^2}\right],$$

$$y = \frac{\omega}{n\sqrt{2\delta\omega^2}}. \quad (11)$$

The results of the numerical calculations for a fixed number of particles and different revolution frequency spreads (longitudinal temperatures) are shown in Fig. 1. One can see that with decreasing beam temperature, two peaks, corresponding to two waves, appear. The position of the peaks has a rather weak dependence on the beam temperature. With decreasing temperature, the peaks become sharper and approach the positions determined by the value of the coherent shift.

As has been previously reported [5], ASTRID was used to first study uncooled beam using Schottky and laser diagnostics. The Schottky spectra, which were strongly
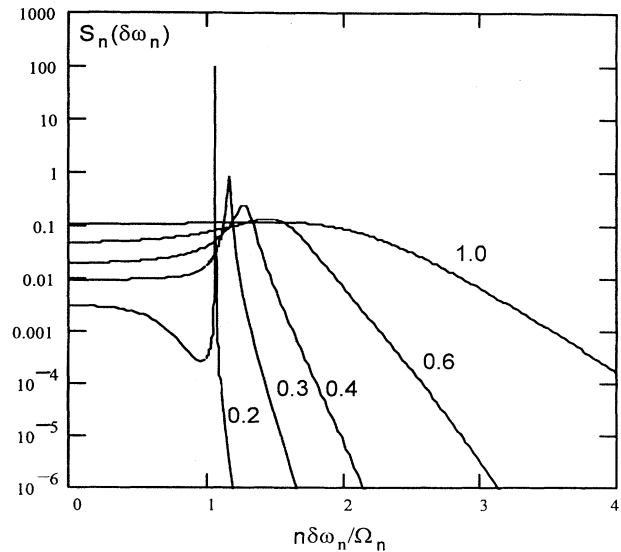

FIG. 1. Dependence of the spectral density on frequency for different particle momentum spreads. The numbers on the plot are values of $n\sqrt{\delta\omega^2}/\Omega_n$.

TABLE I. Velocity spread of an uncooled beam for various times after injection, inferred from Schottky spectra and measured by LIF.

Time (s)	Sound velocity $v_s \equiv \Omega \bar{R}$ (m/s)	$\sqrt{\overline{\delta v^2}}$ for Schottky measurements (m/s)	$\sqrt{\overline{\delta v^2}}$ for LIF measurements (m/s)
0.5	744±7	518±36	481±5
0.8	685±11	546±37	512±22
1.0	649±12	588±39	536±27

distorted by particle interactions, were analyzed using Eq. (11) above. The extracted velocity spreads were then compared to direct measurements of the velocity distribution, which were carried out using a laser-induced fluorescence (LIF) technique [5]. Some results are shown in Table I. Although LIF measurements systematically give lower values than the Schottky analysis, the two agree to within the experimental error (see also the next section for details of the experiment). These measurements confirm the validity of the model described above for Gaussian velocity distribution.

III. ANOMALOUS BEHAVIOR OF SCHOTTKY NOISE IN A LASER-COOLED BEAM

The analysis given below is based on the experimental results obtained in the laser-cooling experiments [5] carried out at the ASTRID storage ring. The relevant parameters for the cooling experiments are presented in Table II. All measurements of the Schottky noise were done at the 23rd revolution frequency harmonic of about 514 kHz.

To understand the difference between the behavior of Schottky noise in laser and electron cooling, we need to consider the process of laser cooling in more detail. The cooling force is created by two counterpropagating laser beams [5]. Because the natural width of the absorption line can be very small compared to the laser detuning, the cooling force often consists of two separate peaks associated with two lasers. The distance between the peaks is determined by the detuning of the laser frequencies. An example of such a cooling force is shown in Fig. 2.

To cool the beam, the laser detuning is initially set so that the force peaks are located outside of the particle distribution function. Then as the lasers are scanned in frequency the particles are pushed by the cooling force to
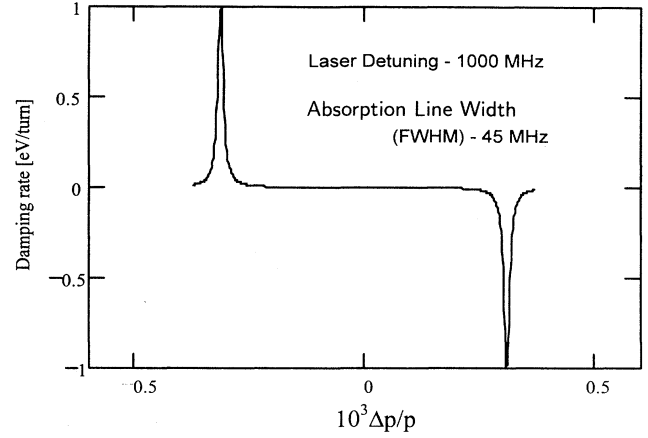

FIG. 2. Calculated drag force for laser detuning of 1000 MHz.

the center of the distribution function. During scanning, such a cooling process produces a particle distribution function that has very sharp edges and is distinct from a Gaussian in that it has virtually no tails. Examples of experimental measurements of particle distribution functions and Schottky spectra at different stages of cooling are shown in Fig. 3.

As one can see from Fig. 3, the behavior of Schottky noise in a laser-cooled beam is significantly different from that described in the above theory. Although, as expected, two peaks appear in the spectra during beam cooling, there are three important distinctions. First, just after switching on the beam cooling, the integral of the spectral density around the 23rd revolution harmonic, $\langle A_n^2 \rangle|_{n=23}$, increases rapidly with decreasing momentum spread and reaches a value higher by two orders of magnitude than that observed without cooling (Fig. 4). As scanning proceeds, its value decreases and has roughly the same value as without cooling at the very end of the process, when the beam momentum spread is more than ten times smaller. Second, the splitting between peaks depends strongly on the momentum spread (Fig. 5), while from the theory for a Gaussian beam this dependence is expected to be rather weak. Finally, the heights of the two peaks are widely different. Figures 3–5 demonstrate these described distinctions.

The absence of tails in the distribution function is the clue to the understanding of the strange behavior of the

TABLE II. ASTRID storage ring parameters.

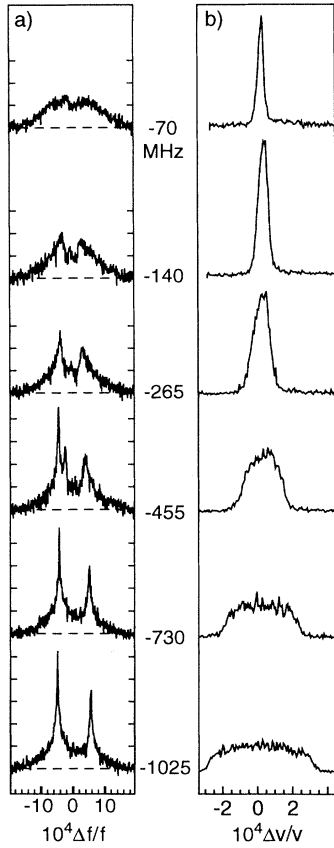|	
Ion kinetic energy	100 keV
Ions	$^{24}Mg^+$
Beam current	2–4 μA
Number of particles	$(5.6-11.2) \times 10^8$
Circumference	40 m
Revolution frequency	22.3 kHz
Betatron tunes v_x, v_z	2.21,2.64
Momentum compaction factor α	0.07
Laser wave lengths, copropagating, counterpropagating	≈278.8,280.4 nm
Laser power	20–40 mW

FIG. 3. (a) Schottky spectra measured at various detunings (shown between figures) during laser cooling. Dashed lines indicate the noise floor of the measurement; each vertical tick mark is one decade in relative power (10 dB). (b) The corresponding velocity distribution, measured by laser-induced fluorescence. Each spectrum contains about 10^3 fluorescence counts.
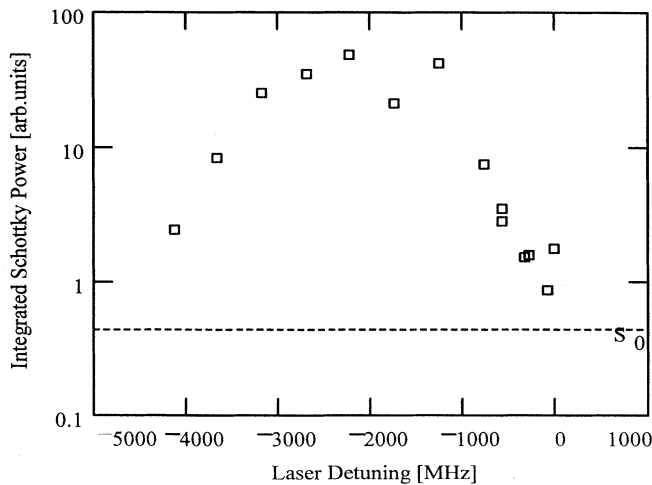

FIG. 4. Dependence of the integral of spectral density around the 23rd harmonic on the laser detuning. Dotted line shows value without laser cooling.
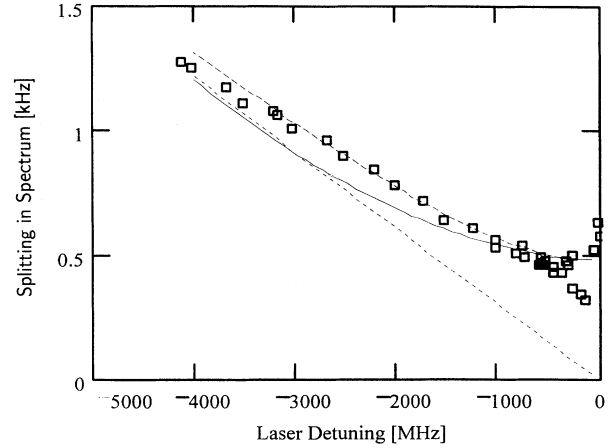

FIG. 5. Dependence of splitting between the peaks in the noise spectra on the detuning of the lasers. The dotted line shows the value of the laser detuning expressed in terms of the shift of the revolution harmonic that was used for measurements. Dashed and solid lines show the theory predictions for the rectangular distribution function and for the distribution function described in Eq. (12), respectively.

Schottky signal described above. As will be seen, the reason for the great amplification of the noise is the disappearance of Landau damping.

IV. BEAM PERMITTIVITY WITHOUT FRICTION

In order to simplify calculations we will first neglect the cooling force. This is justified by the fact that most of the particles experience virtually no force at the first stage of the cooling, when the detuning is large. The particles are just pushed by the cooling force towards the center of the distribution function, where they stay without friction. Their velocities will not change in the absence of diffusion. To estimate the effect of the drag force, we can compare the damping decrement at the center of the distribution function (zero relative velocity), $\lambda = (1/M)\partial F/\partial v|_{v=0}$, and the coherent shift. The results of such a comparison for the parameters of the experiment are shown in Fig. 6. One can see that when the detuning of the lasers is more than ~ 500 MHz, the decrement is at least two orders of magnitude smaller than the coherent shift, and the cooling force can be neglected in the first approximation.

Thus we consider a model where we neglect the friction force and use a simple expression for the distribution function, which should approximate the results of the measurements better than the Gaussian distribution. To calculate the beam permittivity we will use the following normalized distribution function:

$$f_\omega(\omega) = \begin{cases} \dfrac{45}{64\omega_b}\left[1 - 2\left[\dfrac{\omega}{\omega_b}\right]^4 + \left[\dfrac{\omega}{\omega_b}\right]^8\right], & |\omega| \leq \omega_b, \\ 0, & |\omega| \geq \omega_b. \end{cases}$$
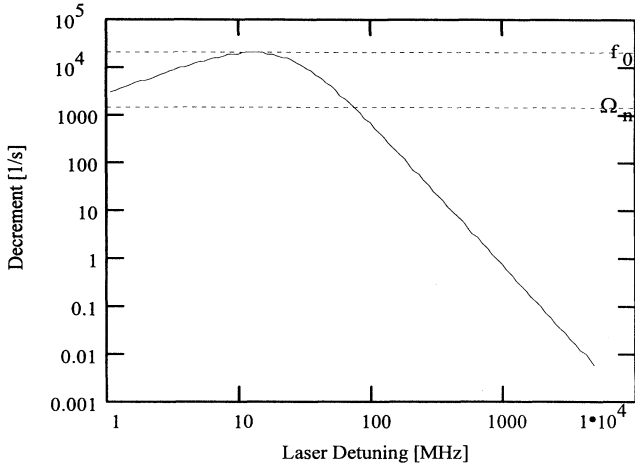
(12)

FIG. 6. Dependence of the damping decrement at zero relative velocity on the detuning of lasers for the parameters of the ASTRID storage ring. The revolution frequency and the coherent shift for the 23rd harmonic are shown by dashed lines.

Here $2\omega_b$ is equal to the full width of the distribution function. This function has much steeper edges than a Gaussian function and represents a much better approximation to the results of the measurements. Figure 7 shows the fits of this function and the Gaussian distribution to the experimentally measured distribution for a laser detuning of 1025 MHz. As one can see, for this particular measurement there is very good agreement with the suggested functional shape, although for most cases the measured distribution functions have even steeper edges and the agreement is not quite as good. The vertical lines in the figure show the positions where the particles are in resonance with the lasers.
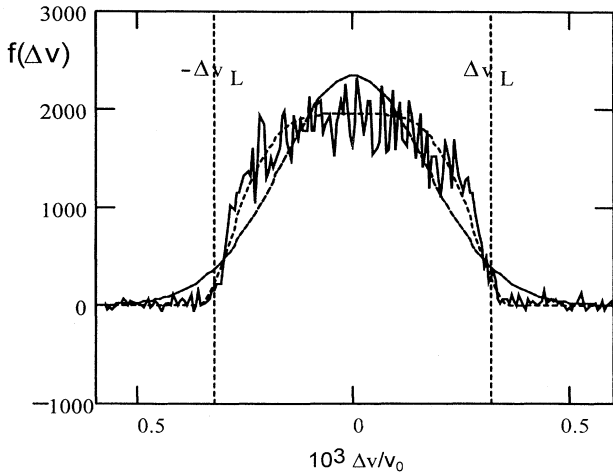

FIG. 7. Measured velocity distribution function for laser detuning of 1025 MHz. Also shown are fits to this function: Gaussian distribution (dashed line) and the distribution described in Eq. (12) (dotted line). Vertical dotted lines show the velocities where ions are in resonance with laser radiation. Relative velocity and revolution spreads are related by $\delta\omega_n/(n\omega_0)=(1-\alpha)\Delta v/v_0$.

Substituting Eq. (12) into Eq. (5) and performing the calculation, we finally find that the permittivity is given by

$$\varepsilon_n(\omega)=1+\frac{45\Omega_n^2}{8n^2\omega_b^2}\left[\frac{8}{21}+\frac{8}{5}y^2-\frac{2}{3}y^4-2y^6\right.$$

$$\left.-y^3(y^4-1)\ln\frac{y-1}{y+1}\right], \quad y=\frac{\omega}{n\omega_b}.$$

$$(13)$$

For $\omega_b\leq 2.13\Omega_n/n$ the equation $\mathrm{Re}[\varepsilon_n(\omega_r)]=0$ has two real positive roots (see Fig. 8). The solution for the larger root can be approximated as

$$\omega_r=n\omega_b\left[\frac{\Omega_n}{n\omega_b}+0.282\left[\frac{n\omega_b}{\Omega_n}\right]^{0.8}\right], \quad n\omega_b\leq 2.13\Omega_n$$

$$(14)$$

to an accuracy of about 1%. Taking into account that for $n\omega_b\leq 1.96\Omega_n$ the imaginary part of the permittivity is also equal to zero at these points, we find that ε becomes zero, too, i.e., the dispersion equation $\varepsilon_n(\omega_r)=0$ has real roots for $n\omega_b\leq 1.96\Omega_n$. These frequencies, where ε becomes zero, determine the positions of peaks in the spectra. The solid line in Fig. 5 shows the splitting between peaks calculated from Eq. (14). As one can see, the peak positions approach the coherent shift only for the case when $n\omega_b\ll\Omega_n$. To test how strongly this result depends on a particular form of the distribution function we also calculated the beam permittivity for a rectangular distribution function. (The use of this function is not fully correct for frequencies near the distribution function edge, where ε goes to infinity. We can neglect this in our consideration because the frequencies in which we are interested are well outside of this point.) The results of these calculations are shown by the dashed line in Fig. 5. As one can see, the behavior of the curve is also in close agreement with the experimental results. Thus we can conclude that, in contrast to a Gaussian distribu-
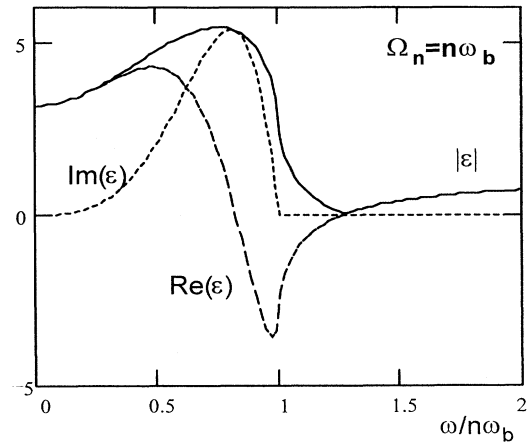

FIG. 8. Dependence of beam permittivity on frequency for the distribution described in Eq. (12), $\Omega_n/n\omega_b=1$.

tion function, the distribution functions with steep edges reproduce the dependence of the splitting between peaks, which has been observed in experiments.

At zero relative frequency we can neglect the influence of the tails. According to Eq. (13) the beam permittivity at zero frequency is

$$\varepsilon(0) \approx 1 + \frac{45}{21} \frac{\Omega_n^2}{n^2 \omega_b^2} . \tag{15}$$

Then the noise spectral density at zero frequency is equal to

$$S(0) \approx \frac{45N}{64n\omega_b} \frac{1}{\left[1 + \dfrac{45}{21} \dfrac{\Omega_n^2}{n^2 \omega_b^2}\right]^2} . \tag{16}$$

A comparison of the measured data and the predictions of Eq. (16) is shown in Fig. 9. Taking into account that the height of the peaks changes by more than a factor of 1000 over the range of laser dutunings, one can appreciate that there is good agreement between theory and experiment, at least for large laser detuning (more than 500 MHz), where we can neglect the cooling force.

V. INFLUENCE OF TAILS ON SCHOTTKY SPECTRA

Although we obtain the right prediction for the splitting between the zeros of the permittivity, the model does not yet predict the existence of peaks in the noise spectrum, since the distribution function is equal to zero at the frequencies corresponding to the zeros of $\varepsilon_n(\omega)$. In reality, there must be small tails in the distribution function that will supply particles to these regions. Although there is a small number of particles, the noise spectral
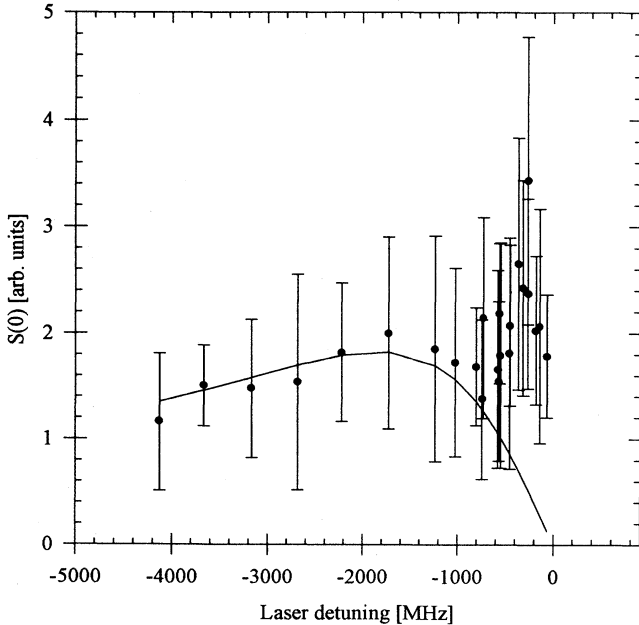

FIG. 9. Dependence of the noise spectral density at zero relative frequency on laser detuning.

power becomes very large because ε is very small.

We can consider that the particle distribution function consists of two parts: the functions for the central part and for the tails,

$$f_s = f + \delta f . \tag{17}$$

Because only a small number of particles are located in the tails, one can neglect their contribution to ε for all frequencies, except when ε becomes zero. Here one can also neglect the contribution of the tails to the real part of ε because it slightly changes the positions of the peaks but does not change their heights. Thus we can let

$$\varepsilon_n(\omega) = 1 + \frac{\Omega_n^2}{n} \int_{-\infty}^{\infty} \frac{\partial (f + \delta f)/\partial \omega'}{\omega - n\omega' - i\Delta} d\omega'$$

$$\approx \varepsilon_{0n}(\omega) + \pi i \frac{\Omega_n^2}{n^2} \frac{\partial \delta f}{\partial \omega} \bigg|_{\omega' = \omega/n} , \tag{18}$$

where $\varepsilon_{0n}(\omega)$ is the beam permittivity without the tails. Let ω_r be the real root of the dispersion equation $\varepsilon_{0n}(\omega_r) = 0$; then we can expand ε in a Taylor series in the vicinity of ω_r,

$$\varepsilon_n(\omega) \approx \frac{\partial \varepsilon_{0n}}{\partial \omega} \bigg|_{\omega = \omega_r} (\omega - \omega_r) + \pi i \frac{\Omega_n^2}{n^2} \frac{\partial \delta f}{\partial \omega} \bigg|_{\omega = \omega_r/n} . \tag{19}$$

If $\partial \delta f / \partial \omega |_{\omega = \omega_r} < 0$, then the system is stable and we can use Eq. (4). Substituting Eq. (19) into Eq. (4) we get an equation describing the spectral density near the peak,

$$S_n^{\text{peak}}(\delta\omega)$$
$$= \frac{N}{n} \frac{\delta f(\omega_r/n)}{\left[\dfrac{\partial \varepsilon_{0n}}{\partial \omega}\bigg|_{\omega=\omega_r} \delta\omega\right]^2 + \left[\pi \dfrac{\Omega_n^2}{n^2} \dfrac{\partial \delta f}{\partial \omega}\bigg|_{\omega=\omega_r/n}\right]^2} ,$$

$$\delta\omega = \omega - n\omega_0 \pm \omega_r . \tag{20}$$

For a cold beam, $\omega_b \ll \Omega_n$, these peaks produce the main contribution to the harmonic amplitude. Then, to find the total integral around nth harmonic we use

$$\langle A_n^2 \rangle \approx 2 \int_{-\infty}^{\infty} S_n^{\text{peak}}(\omega) d\omega$$

$$= \frac{2Nn\delta f(\omega_r/n)}{\Omega_n^2 \left|\dfrac{\partial \varepsilon_{0n}}{\partial \omega}\right|_{\omega=\omega_r} \left|\dfrac{\partial \delta f}{\partial \omega}\right|_{\omega=\omega_r/n}} . \tag{21}$$

The factor of 2 appears in Eq. (21) because there are two peaks in the spectrum. One can see that if the derivative of the distribution function in the tails goes to zero, the Landau damping disappears and the spectral density goes to infinity. For a positive derivative the system becomes unstable.

VI. DIFFUSION AND THE ORIGINATION OF THE TAILS

For particles in the tails, which are outside the range between the cooling force peaks, the cooling force decreases rapidly with velocity. This implies that if a particle diffuses out from the core it will stay in the tail for a

long time. Thus, even small particle diffusion can produce large tails in the distribution function.

There are two main mechanisms that produce tails. They are interbeam scattering and collisions with residual gas. Although the diffusion due to multiple small angle scattering is usually the dominant effect, it does not produce large tails because of the effective barrier of the strong friction force, which confines particles to a small velocity range. However, in the event of an energetic single scattering a particle can jump past this barrier to the tail, where the friction force is very small.

For the conditions of the laser-cooling experiment described here, the single collision intrabeam scattering (Touschek effect) is the dominant mechanism for populating the tails. For an estimate we can consider the storage ring in the smooth approximation, with equal horizontal and vertical sizes and velocity spreads. Then, if the longitudinal temperature is much smaller than the transverse one, the following expression can be used to calculate the number of particles scattered with longitudinal velocity more than v (Touschek lifetime) [10]:

$$\frac{1}{N}\frac{dN}{dt} = \frac{e^4 N}{4\sqrt{\pi}M^2 v^2 \bar{v}_x \bar{R}\sigma^2}$$

$$\times \left[\frac{\sqrt{\pi}}{2}(1+2\Delta^2)\left[1-\frac{2}{\sqrt{\pi}}\int_0^\Delta e^{-x^2}dx\right]\right.$$

$$\left. -\Delta e^{-\Delta^2}\right].\tag{22}$$

Here N is the number of particles in the beam, e and M are the charge and mass of the ion, $\bar{v}_x$ is the rms transverse velocity, σ is the rms beam radius, $\bar{R}$ is the mean radius of the storage ring, and $\Delta = v/\bar{v}_x$. Differentiating Eq. (22) with respect to v, one can calculate the flux of particles into the tails of the distribution function, $d^2N/dtdv$. Due to the cooling force these particles will be decelerated towards the center of the distribution. Figure 10 shows the results of a numerical calculation of
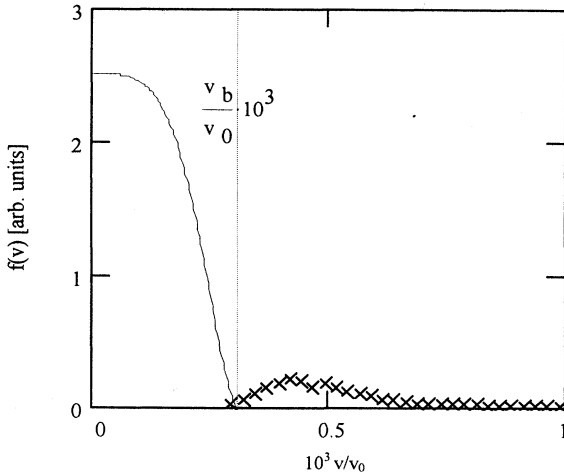

FIG. 10. Simulation result of the particle density distribution in the tails for parameters of the laser-cooling experiment with ^{24}Mg$^+$; $I_p = 2\,\mu$A, $\sigma = 3$ mm, $\bar{v}_x/v_0 = 10^{-3}$. Crosses, density distribution in tails; solid line, initial density distribution.

the distribution function for the tails, considering only the cooling force and Touschek scattering. One can see that because of the drag force the derivative of the distribution function is positive for velocities in the range $\approx (1-1.5)v_b$, where v_b is the velocity when a particle is in resonance with the laser radiation. If the velocity corresponding to the coherent shift, $R\Omega_n/n$, is in this range, the beam becomes unstable and longitudinal coherent motion will be excited in the beam. Note that in this calculation we neglected multiple intrabeam scattering, which will smoothen the distribution presented in Fig. 10 and will possibly exclude the positive derivative and the beam instability.

VII. INFLUENCE OF THE FRICTION FORCE ON THE SCHOTTKY SPECTRUM

The cooling force changes the beam permittivity. Although for the general case of a nonlinear friction force and a non-Gaussian distribution function it is impossible to perform an analytical calculation of the permittivity, some simple formulas can give reasonable accuracy in many practical cases.

It was found in Ref. [3] that in the limit of a cold beam and strong cooling the permittivity is

$$\varepsilon_n(\omega) \approx 1 - \frac{\Omega_n^2}{\omega(\omega - i\lambda)},\tag{23}$$

where λ is the single particle cooling decrement. On the other hand, if the beam is sufficiently cold, $n^2\delta\omega^2 \ll \Omega_n^2$, then Eq. (5) implies that for frequencies $\omega^2 \gg n^2\delta\omega^2$, the permittivity is equal to

$$\varepsilon_n(\omega) \approx 1 - \frac{\Omega_n^2}{\omega^2} + \pi i \frac{\Omega_n^2}{n^2}\frac{\partial f}{\partial\omega}\bigg|_{\omega/n}.\tag{24}$$

The last term corresponds to the contribution from Landau damping. If the Landau decrement is small in comparison to the coherent shift, these two equations can be combined,

$$\varepsilon_n(\omega) \approx 1 - \frac{\Omega_n^2}{\omega(\omega - i\lambda)} + \pi i \frac{\Omega_n^2}{n^2}\frac{\partial f}{\partial\omega}\bigg|_{\omega/n},$$

$$\Omega_n^2 \gg n^2\overline{\delta\omega^2}, \quad \omega^2 \gg n^2\overline{\delta\omega^2},\tag{25}$$

which is justified for all practical cases of a cold beam. For a nonlinear friction force, $F(v)$, we can express λ as an average over the particle distribution function,

$$\lambda = -\frac{1}{M}\int_{-\infty}^\infty \frac{\partial F}{\partial v}f(v)dv.\tag{26}$$

In the vicinity of the peak in spectral density, $\omega \approx \Omega_n$, we can expand Eq. (25) into

$$\varepsilon_n(\omega) \approx 1 - \frac{\Omega_n^2}{\omega^2} + i\frac{\lambda_s}{\Omega_n},\tag{27}$$

where the total decrement is

$$\lambda_s = \lambda - \pi\frac{\Omega_n^3}{n^2}\frac{\partial f}{\partial\omega}\bigg|_{\Omega_n/n}.\tag{28}$$

Taking into account that the coherent shift is proportional to n, one can see that the contribution of Landau damping also grows proportionally to n while the contribution of laser damping does not depend on n. Using Eqs. (4) and (27) one can obtain the spectral density around the peak

$$S_n^{\text{peak}}(\delta\omega) = \frac{Nf(\Omega_n/n)}{n} \frac{\Omega_n^2}{4\delta\omega^2 + \lambda_s^2}, \quad \delta\omega = \omega - n\omega_0 \pm \omega_r .$$

(29)

Thus in the case of a cold beam, the spectral density of fluctuations is determined by three parameters. They are the coherent shift Ω_n, the coherent decrement λ_s, and the value of the distribution function at the resonant frequency $f(\Omega_n/n)$. It is important to note that measurements at different harmonics would allow an identification of the separate contributions from Landau damping and external (laser or electron) damping.

The dependencies on laser detuning calculated from measurements are shown in Figs. 11 and 12 for the distribution function values at the resonant point $df/d\omega|_{\Omega_n/n}$ and for the damping decrement. Taking into account that in Touschek scattering a particle cannot get a longitudinal velocity kick much larger than the rms transverse velocity, and assuming that the particles in the tails are evenly distributed in a velocity range determined by the transverse velocity spread $-\bar{v}_x \leq v \leq \bar{v}_x$, we can estimate the total number of particles in the tails. The results of such an estimate are shown in Fig. 12. The scale on the right-hand side of the plot shows an estimate of the percentage of particles in the tails, calculated with the following formula:

$$\Delta N/N = 2f(\Omega_n/n)\bar{v}_x/R .$$

(30)

One can see that there is a good qualitative agreement with the simulation results presented in Sec. VI. Unfortunately, the accuracy of the measured beam parameters
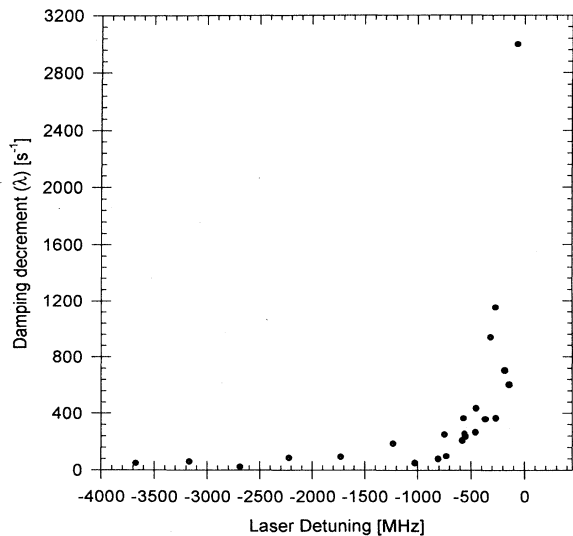

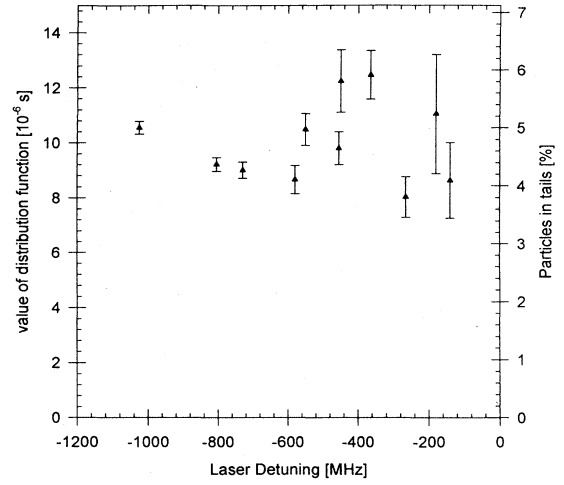FIG. 11. Damping decrement as a function of laser detuning.

FIG. 12. Value of the distribution function at the frequency of the Schottky peak as a function of laser detuning.

is not currently sufficient to do a more accurate comparison.

VIII. DISCUSSION

The ASTRID data that are analyzed in this paper represent simultaneous measurements of both the Schottky spectra and the velocity distributions in a very cold beam [6]. In general, good agreement was obtained between experimental measurements and the proposed theoretical model. It should be noted that at intermediate laser detuning, when the peaks in the spectrum become very narrow and large, their width is mostly determined by the resolution of the fast Fourier transform (FFT). This probably explains the difference between the measured Schottky spectra and the theoretical analysis (see Fig. 13), which predicts a bell-shaped curve in the spectrum center and more narrow peaks. Although the friction force, which also produces broadening, was neglected in the theoretical curve of Fig. 13, its effect is not very large, because as can be seen from the figure, the peak width is determined by the FFT resolution. Numerical experiments carried out on the FFT of an ideal sinusoid exhibit behavior almost identical to the measured spectral density in the peak.

The experimental results from ASTRID illustrate that the model for Schottky noise based upon a Gaussian velocity distribution is not applicable to a laser-cooled beam during cooling. The model presented here emphasizes the importance of the detailed shape of the velocity distribution in determining the fluctuation spectrum. In particular, the tails of the velocity distribution play an important role. In general, particle beams in storage rings often have an asymmetric velocity distribution due to energy loss in the rest gas, and they may also have long, non-Gaussian tails. The analysis presented here may thus have a wider application, for example to electron-cooled beams.

In previous works, the difference in peak heights in the Schottky spectra of electron-cooled beams was attributed
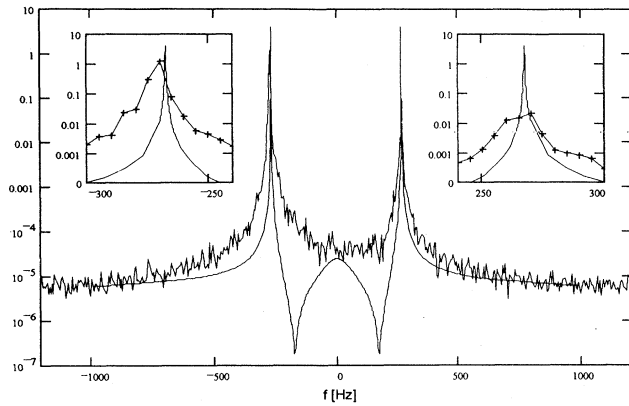
FIG. 13. Comparison of the experimentally measured Schottky spectrum for laser detuning of 1025 MHz and the theory prediction. The distribution function is linearly combined from two parts: the core and the tails. The core is described by Eq. (12) and its plot is shown in Fig. 7. The tails include 15% of the particles and are described by Gaussian distribution with a temperature equal to the transverse beam temperature, so that $\sqrt{\delta v^2}/v_0 = 2.7 \times 10^{-3}$. The friction force was neglected in the theory. Insets show the peaks on a smaller scale.

to the real part of the storage ring impedance [9], which causes an increase of the lower peak and a decrease of the upper peak. Such a difference has been observed in many experiments, but it should be noted that in the case of the laser-cooled beam in ASTRID, the intensity of both peaks was strongly increased (compared to a Gaussian beam), which implies that the effect of the tails deter-

mines the main contribution to Schottky noise. The effect of the tails may also be responsible for the different heights of the peaks in the case of electron cooling, because the inelastic scattering on residual gas atoms produces an asymmetry in the tails of the velocity distribution; it creates a tail at low velocity but cannot influence the tail at high velocity. Like the real part of the ring impedance, it causes an increase of the lower peak height. The effects of these two possible mechanisms could easily be distinguished by measurements at different gas pressures, which should have a strong effect on the tails but cannot, of course, change the ring impedance. For a beam cooled by counterpropagating laser beams, an asymmetry may also arise due to differences in laser powers or spatial overlap of the laser and ion beams.

Although the Schottky spectra of laser-cooled beams appear to be very complicated, this paper demonstrates that quantitative information about beam parameters can be extracted from them. In the future, it is very important to do measurements on different harmonics of the revolution frequency, because both the ring impedance from the vacuum chamber walls and the effect of the drag force depend strongly on harmonic number. It is hoped that the theoretical model presented here will prove valuable in diagnosing the behavior of very cold beams that are not in equilibrium.

ACKNOWLEDGMENTS

[1] H. Koziol, in *Beam Diagnostics for Accelerators*, Proceedings of the CERN Accelerator School, Fifth General Accelerator Physics Course, edited by S. Turner (CERN, Geneva, 1994).

[2] Yu. L. Klimontovich, *Statistical Theory of Non Equilibrium Processes in Plasma* (Moscow State University, Moscow, 1964) (in Russian).

[3] V. V. Parkhomchuk and D. V. Pestrikov, Zh. Tekh. Fiz. **50**, 1411 (1980) [Sov. Phys. Tech. Phys. **25**, 818 (1980)].

[4] E. N. Dementiev *et al.*, Zh. Tekh. Fiz. **50**, 1717 (1980) [Sov. Phys. Tech. Phys. **25**, 1001 (1980)].

[5] J. S. Hangst *et al.*, Phys. Rev. Lett. **74**, 86 (1995).

[6] J.-L. Laclare, in *Coasting Beam Longitudinal Coherent Instabilities*, Proceedings of the CERN Accelerator School; Fifth General Accelerator Physics Course, edited by R. Calabrese and L. Tecchio (CERN, Geneva, 1994).

[7] A. I. Akhiezer, *Plasma Electrodynamics* (Pergamon, New York, 1975).

[8] N. S. Dikansky and D. V. Pestrikov, *Physics of the Intense Beams in Storage Rings* (Nauka, Novosibirsk, Moscow, 1989) (in Russian).

[9] D. V. Pestrikov, in *Proceedings of the Workshop "Electron Cooling and New Cooling Techniques,"* Legnaro, Italy, *1990*, edited by Editor (World Scientific, Singapore, 1991).

[10] H. Brook, Accélérateurs Circulaires de Particules (Presses Universitaires de France, Paris, 1966).